

Visible and near-infrared spectral survey of Martian meteorites stored at the National Institute of Polar Research

Takahiro Hiroi^{a,b,*}, Hiroshi Kaiden^{a,c}, Keiji Misawa^{a,c}, Takafumi Niihara^{c,1},
Hideyasu Kojima^{a,c}, Sho Sasaki^d

^a Antarctic Meteorite Center, National Institute of Polar Research, 10-3 Midori-cho, Tachikawa, Tokyo 190-8518, Japan

^b Department of Geological Sciences, Brown University, Providence, RI 02912, USA

^c Department of Polar Science, The Graduate University for Advanced Studies, 10-3 Midori-cho, Tachikawa, Tokyo 190-8518, Japan

^d RISE Project, National Observatory of Japan, Mizusawa-ku, Oshu, Iwate 023-0861, Japan

Received 26 August 2010; revised 15 April 2011; accepted 7 June 2011

Available online 1 July 2011

Abstract

Martian meteorite chip samples stored at the National Institute of Polar Research (NIPR) have been studied by a visible and near-infrared (VNIR) spectrometer. Measured spots are about 3×2 mm in size, which are clearly marked on photographs of the meteorite chips. Rock types and approximate mineral compositions of studied meteorites have been identified or obtained through this spectral survey with no sample preparation required. This study demonstrates that this kind of spectral survey is effective in classifying and describing Martian meteorites, and that such a VNIR spectrometer on a Mars rover would be useful for identifying these kinds of unaltered Mars rocks. Further studies which utilize a smaller spot size are desired for improving the accuracy of identifying the clasts and mineral phases in the rocks.

© 2011 Elsevier B.V. and NIPR. All rights reserved.

Keywords: Meteorite; Mars; Reflectance; Spectroscopy; Exploration

1. Introduction

Martian meteorites have been serving as hands-on samples of Mars for petrologists and other planetary scientists to study the composition and evolution of Mars. Spacecraft and rovers to Mars further enhanced our knowledge of the red planet by providing Martian surface and rock compositions, primarily via their thermal emission spectra (*e.g.*, Schueller *et al.*, 2005).

* Corresponding author. Department of Geological Sciences, Brown University, Providence, RI 02912, USA.

E-mail address: takahiro_hiroi@brown.edu (T. Hiroi).

¹ Present address. Lunar and Planetary Institute, 3600 Bay Area Blvd., Houston, Texas 77058, USA.

However, the lack of a near-infrared (NIR) spectrometer on Mars Exploration Rovers (MERs) prevented us from utilizing one of the most useful wavelength regions in identifying the mineral compositions of rocks and their clasts. Such measurements could have linked rocks on Mars with Martian meteorite samples and enhanced our knowledge on their original locations and formation environments.

There are studies on spectral properties of individual mineral components of Martian meteorites (*e.g.*, Dyar *et al.*, 2011). In spite of usefulness and depth of such studies, mineral separation on Mars and even in laboratories is often challenging. For future application to Mars rovers and easy characterization of Martian

meteorites, reflectance spectral measurements of small areas on the surfaces of those meteorite samples are desired. That would also enhance the value of our Martian meteorite collections.

For the above reasons, we have conducted a visible and near-infrared (VNIR) spectral survey of Martian meteorites collected or owned by the National Institute of Polar Research (NIPR).

2. Experimental

Samples of Antarctic Martian meteorites collected by the National Institute of Polar Research (NIPR) and the Nakhla meteorite were considered for this study. Out of the available eleven Antarctic Martian meteorites, six subsamples were selected along with Nakhla for this study by considering freshness and texture (having a naturally broken surface) and suggested pairing. The considered meteorite samples are listed in Table 1, and the photographs of eleven selected samples are shown in Fig. 1 with nine measured spots (about 3×2 mm in size) indicated. Those spots were selected as representative of either the average or an end-member of each sample.

Bidirectional UV-visible-NIR diffuse reflectance spectra of those spots were obtained using a diffuse reflectance spectrometer manufactured by Bunkou-keiki installed in Mizusawa campus of the National Astronomical Observatory of Japan (NAOJ). The measurement geometry was set to 30° incidence and 0° emergence angles in order to avoid specular reflection and facilitate easy comparison with other spectral datasets such as the RELAB database (Pieters, 1983; Pieters and Hiroi, 2004). The wavelength range was 250–2500 nm, and data were recorded at every 5 nm. All spectra were measured relative to Spectralon

purchased from Labsphere, a near perfect diffuse reflector over this wavelength region, and the relative reflectances were corrected for the absolute reflectance of Spectralon, especially for the prominent absorption bands starting at around 2150 nm in wavelength.

2.1. Linear deconvolution method

Because identifying the mineral species and their abundances in each measured spot is a major objective of this study, a simple linear deconvolution using negative coefficients (extrapolation) was applied to some sets of spectra to derive their end-member spectra. To be more specific, if two measured spots A and B contain mineral components 1 and 2, their reflectances R_A and R_B can be expressed as:

$$R_A = c_A R_1 + (1 - c_A) R_2 \quad (1)$$

$$R_B = c_B R_1 + (1 - c_B) R_2 \quad (2)$$

where R_1 and R_2 denote reflectances of mineral components 1 and 2, respectively, and coefficients c_A and c_B denote the areal contents of mineral component 1 on spots A and B, respectively. By solving Eq. (1) and (2), reflectances of minerals components 1 and 2 can be obtained:

$$R_1 = \{R_A/(1 - c_A) - R_B/(1 - c_B)\} / \{c_A/(1 - c_A) - c_B/(1 - c_B)\} \quad (3)$$

$$R_2 = \{R_A/c_A - R_B/c_B\} / \{(1 - c_A)/c_A - (1 - c_B)/c_B\} \quad (4)$$

The coefficients c_A and c_B can be roughly estimated from photographs of the measured spots and optimized for the best spectral data (R_1 and R_2) as expected shapes of end-member mineral spectra.

Table 1

List of Antarctic Martian meteorites stored at the National Institute of Polar Research considered for this study.

Meteorite Name	Weight (g)	Classification	Pairing	Subsample No.	Studied Spots
ALH-77005	212.45	Lherzolithic shergottite		86	A, B
Y-793605	16.084	Lherzolithic shergottite		3	A, B
Y 980459	82.46	Olivine-phyric shergottite		12	A
Y 980497	8.713	Olivine-phyric shergottite	Y 980459	42	A
Y 984028	12.342	Lherzolithic shergottite	Y 000027		
Y 000027	9.685	Lherzolithic shergottite		20	A
Y 000047	5.345	Lherzolithic shergottite	Y 000027		
Y 000097	24.484	Lherzolithic shergottite	Y 000027		
Y 000593	13,713	Nakhlite		15	A
Y 000749	1283	Nakhlite	Y 000593		
Y 000802	22	Nakhlite	Y 000593		
Nakhla		Nakhlite		BM1913,26	A

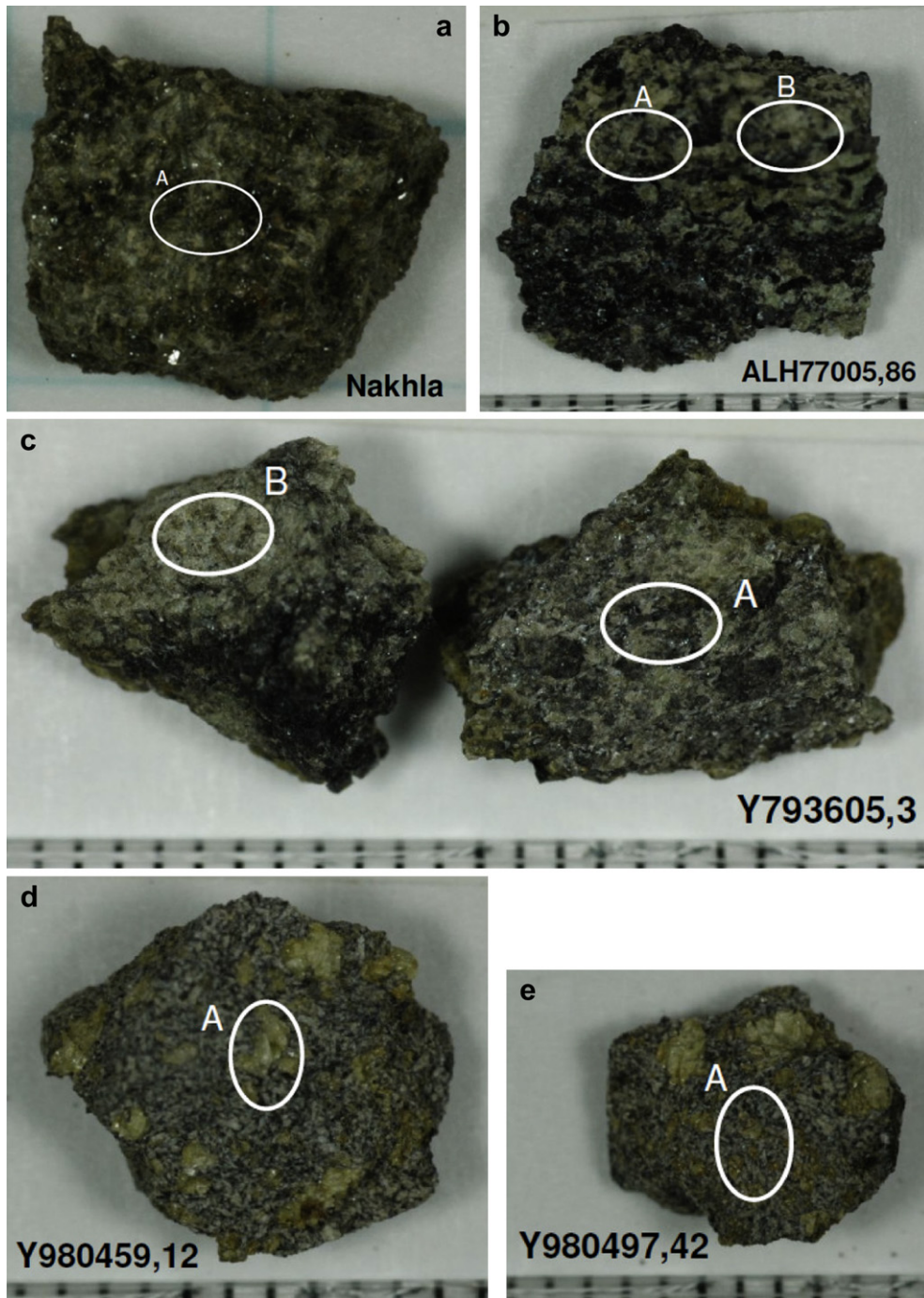


Fig. 1. Photographs of Martian meteorite chips owned by the National Institute of Polar Research (NIPR) indicating the spots of which the reflectance spectra were measured: (a) Nakhla, (b) Allan Hills (ALH)-77005,86, (c) Yamato (Y)-793605,3, (d) Y 980459,12, (e) Y 980497,42, (f) Y 000027,20, and (g) Y 000593,15. Scale ticks have 1 mm intervals, a scale cube is 1 cm in size, and studied spots indicated in white circles are 3×2 mm in size. (For interpretation of the references to color in this figure legend, the reader is referred to the web version of this article.)

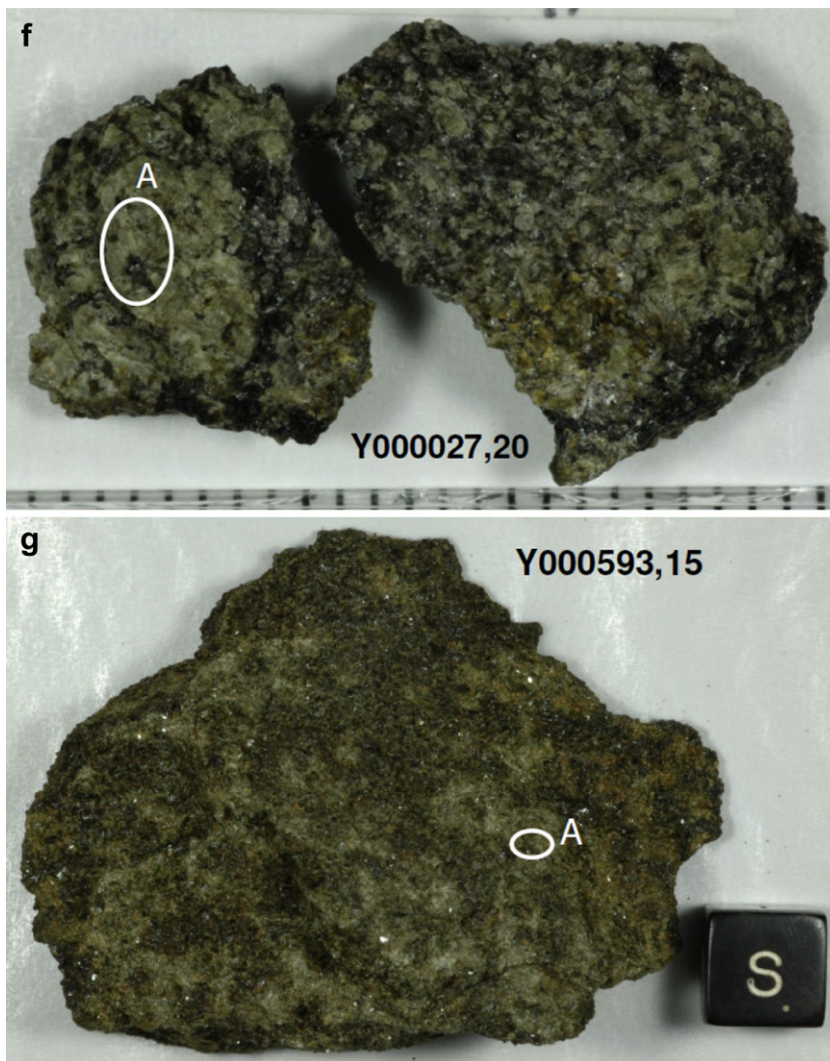


Fig. 1. (continued).

Because this manual method takes intuition and intense efforts and may not yield unique solutions, spectra of selected spots on two Martian meteorite samples have been analyzed by this method. Including the above linear deconvolution, more detailed interpretations of these spectra are given below, according to their petrologic types: lherzolitic shergottite, olivine-phyric shergottite, and clinopyroxenite (Nakhlite), which are easily recognized by their images in Fig. 1.

3. Results

All the reflectance spectra measured on the meteorite sample spots are plotted in Fig. 2. It is

immediately noticed that these spectra show diversity in mineral composition according to the band center positions at around 1 and 2 μm in wavelength, shoulder bands at around 0.85 and 1.25 μm , and the ratio between the 1 and 2 μm band strengths. These are caused by different abundances of low-Ca pyroxene (LCP), high-Ca pyroxene (HCP), olivine, plagioclase, and possibly glass, and variety in their chemical compositions.

Spectral data quality seems high enough for the purpose of this study, except incomplete removal of the absorption feature of Spectralon at around 2.2 μm , especially outstanding with the spectra of Yamato (Y) 980459,12 and Y-793605,3 spot A. Water absorption band at around 1.92 μm is visible especially with the

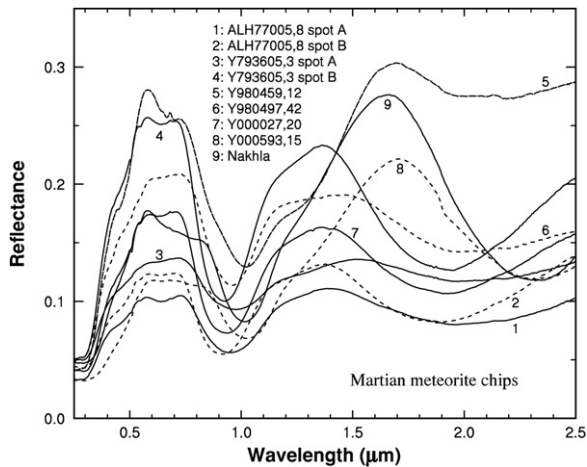


Fig. 2. Bidirectional visible and near-infrared (VNIR) reflectance spectra of the Martian meteorite chip surface spots marked in Fig. 1.

spectra of Y 980459,12, Y-793605,3 spot B, and Y 000593,15, probably due to terrestrial weathering in Antarctica. This alteration feature makes accurate deconvolution analyses such as the modified Gaussian model (MGM) (Sunshine et al., 1990) difficult.

3.1. Lherzolithic shergottites

Shown in Fig. 3 are reflectance spectra of spots on Allan Hills (ALH)-77005, Y-793605, and Y 000027 samples. These spectra are characterized by having two major absorption bands at around 1 and 2 μm , and the apparent band center wavelength ranges (0.91–0.97 and 1.89–1.96 μm) are indicated by two pairs of vertical lines in Fig. 3a. The 2 μm band center wavelength range corresponds to the pyroxene compositional range of Fs 8–44 (Cloutis and Gaffey, 1991). The fact that the 1 μm band center wavelength ranges beyond the longest wavelength than LCPs suggests the presence of either HCP or a significant amount of olivine. Based on the reduced 2 μm band strengths of ALH-77005,86 spot A and Y-793605,3 spot A spectra, olivine should be present by 50% or more in abundance. Because the spots with more dark areas show more olivine-rich spectra, dark areas seem to represent Fe-rich olivine crystals. Kojima et al. (1997), Ikeda (1997), and Mikouchi and Miyamoto (1997) report pyroxene and olivine modal abundances of 50–60 and 35–40%, and Kojima et al. (1997) reports the olivine composition of Fa 31–34. This olivine composition does not support the extrapolated spectral shape of possible olivine end-member in Fig. 3b, and Kojima et al. (1997) describes that a dark melt vein occupies about 40% of the sample.

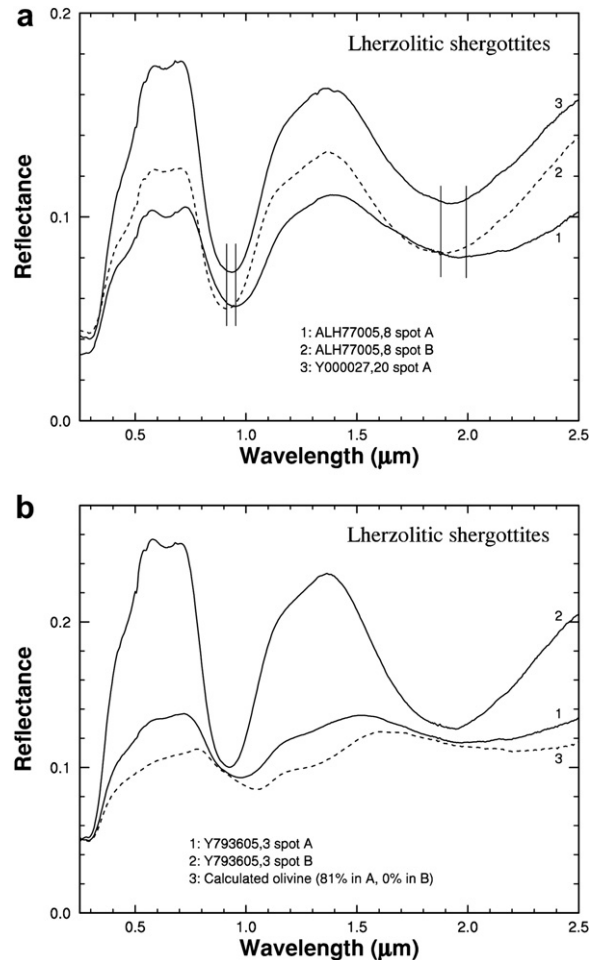


Fig. 3. Comparison of VNIR reflectance spectra of lherzolithic shergottite chip spots, grouped into two. (a) Pyroxene-rich group with two pairs of vertical lines indicating apparent 1 and 2 μm band center wavelength ranges. (b) Y-793605,3 spots and a linearly deconvolved olivine spectrum.

Therefore, it is also possible that this olivine-looking spectrum represents a mixture of olivine and other mineral phases recrystallized from the dark melt.

Because the Y-793605,3 spot A spectrum (Fig. 3b) shows the strongest sign of olivine presence from its 1.25 μm shoulder band and highly reduced 2 μm band, a linear deconvolution was performed to derive the olivine spectrum. Assuming the olivine abundance of 81% in spot A provided a reasonably olivine-looking spectrum (broken line), although it still has a shallow 2 μm band possibly due to HCP and a stronger 1.25 μm shoulder band than typical olivine, possibly due to plagioclase, maskelynite, or glass.

Previous studies (McSween et al., 1979; Mason, 1981; Ma et al., 1981; Lundberg et al., 1990;

Treiman et al., 1994; Wadhwa et al., 1994) report the compositional range of LCP as Fs 20–30, the presence of HCP, and olivine composition of Fa 24–31 and abundance of 44–60%, and maskelynite abundance of 8–12% for ALH-77005. Ikeda (1997) reports that Y-793605 contains 41% olivine, 51% pyroxene, and 7% maskelynite in average based on examining two thin sections. These studies are mostly consistent with the above observations from the spectra of these Iherzolitic shergottite samples.

3.2. Olivine-phyric shergottites

These two meteorite samples, Y 980459,12 and Y 980497,42, look almost identical (Fig. 1), and a spot containing large light-green crystals on Y 980458,12 and a spot without such large crystals on Y 980497,42 were measured. The spectra are plotted in Fig. 4. Based on the fact that Y 980459,12 shows an olivine-rich spectrum, it is clear that the large light-green crystals are olivine. On the other hand, Y 980497,42 shows a more pyroxene-dominant spectrum with a slight influence of olivine seen from its reduced 2 μm band strength.

Based on the above observation, the olivine and pyroxene phase spectra (broken lines) were calculated assuming that the Y 980459 spot has 65% olivine and 35% pyroxene, and the Y 980497 spot has 90% pyroxene and 10% olivine (linear extrapolation). This spectrum is similar to that of synthetic olivine Fa 9.6 (<45 μm in grain size) in terms of the 1.05 μm band

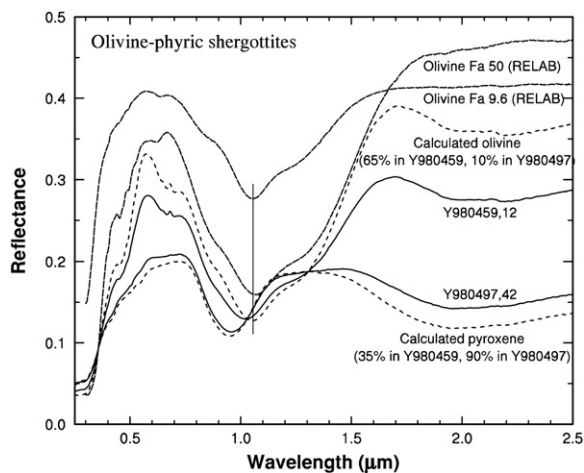


Fig. 4. Comparison of VNIR reflectance spectra of olivine-phyric shergottite chips, their olivine and pyroxene mineral phases (linearly deconvolved), and synthetic olivine (Fa 17.6 and Fa 50) powders (<45 μm in grain size). Reflectance spectra of the synthetic olivine powders were taken from the RELAB database.

center position, although the overall shape is more similar to that of Fa 50, both of which are taken from the RELAB database. Because olivine crystals on these Martian meteorites seem much larger than those measured at RELAB, the shape difference is likely due to grain size difference. Considering the apparent bright green color of olivine crystals on these Martian meteorites, relatively low Fe content of these olivine crystals seems most plausible. The pyroxene 1 μm band center wavelength position of 0.95 μm indicates a composition of Fs 18–52 Wo 30–40 (Cloutis and Gaffey, 1991).

Previous studies (Greshake et al., 2003, 2004; Koizumi et al., 2004; Ikeda, 2003, 2004; Mikouchi et al., 2004) report that Y 980459 contains 48–63% pyroxene, 8–26% olivine, and 30–37% glass, the pyroxene composition is Fs 14–49 Wo 0–38, and olivine is zoned having a compositional range of Fa 14–71. Spectrally estimated Mg number of pyroxene seems mostly consistent with those by previous studies, and that of olivine (Fa 10–50) can also be regarded as consistent, considering relatively a large uncertainty in estimating the composition of olivine from its spectrum.

3.3. Clinopyroxenites (nakhrites)

Plotted in Fig. 5 are reflectance spectra of Nakhla and Y 000593,15 chip samples, along with spectra of Nakhla powder of <100 μm in particle size and synthetic pyroxene (Wo 40 Fs 36) powder of <45 μm

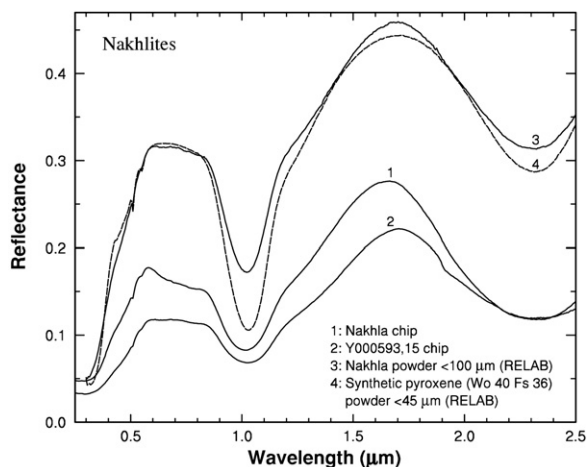


Fig. 5. Comparison of VNIR reflectance spectra of nakhlite samples and synthetic pyroxene (Wo 40 Fs 36) powder. The spectra of Nakhla powder and synthetic pyroxene powder were taken from the RELAB database.

in size, both taken from the RELAB database. Except for the 0.5 and 1.92 μm absorption bands of Y 000593 chip due to terrestrial weathering, Nakhla and Y 000593 show very similar spectra, which are dominated by their augite component.

Previous studies (Mikouchi et al., 2003; Imae et al., 2003) report that Y 000593 is dominated by about 80% pyroxene, and its composition is Wo 40 Fs 20–40 along with a more compositionally diverse group of pyroxenes (Fs 50–70). The augite composition of the spectrum in Fig. 5 is consistent with these studies. Ueda et al. (2003) reports that MGM deconvolutions of the spectra of Nakhla and Y 000593 powder samples also show their similarity in mineral assemblage and composition.

4. Discussion

Spectroscopic observations and analysis performed here cannot fully resolve compositions and modal abundances of different types of pyroxenes and the presence of a significant amount of glass. However, the rock types can be easily identified from the images (Fig. 1) and the spectra (Fig. 2) corresponding to the different clasts or mineral phases in the images. Unlike their powder samples, these meteorite chip surface spectra show more linear combinations of those of different clasts or mineral phases as evident from their images or a calculation performed for the olivine-phyric shergottite spectra (Fig. 4).

If a measured spot is monomineralic or a simple mineral mixture (such as two-pyroxene mixtures), a deconvolution method such as MGM could be applied. In order to do so, the measurement spot should be smaller than the current 3×2 mm in size according to the sizes of clasts and mineral phases of the target rock. Probably a spot of about 1 mm in diameter is ideal in that it is small enough to measure small clasts but large enough to average the surface texture effects although it depends on the scale of the surface roughness which can be controlled if the sample surface can be treated.

The kind of experiments performed in this study is similar to imaging spectroscopy applied to Earth and planetary surfaces through remote sensing by ground-based telescopes or spacecraft, except that we manually select individual areas of interest and the dimension of studied spots is in millimeter scale instead of the meter to kilometer scale in the remote sensing case.

This study is almost exactly what is expected if a VNIR spectrometer is utilized by a Mars rover. Although dusts and weathering products would have to be removed by an abrasive tool for example, almost no other sample preparation is necessary to detect the rock

type and mineralogy of a measured rock and its spots. It is known from Mars remote sensing and spacecraft and rover missions that the red planet has abundant hydrous minerals. The wavelength range employed in this study covers the absorption bands of many hydrous minerals such as carbonates. In addition, there may be many breccias on Mars which may be too weak to survive as Martian meteorites. Because the method of this study can analyze individual clasts of such breccias, it is highly effective in that case as well.

The approach demonstrated here could also be used for the classification and/or description of meteorites. VNIR reflectance spectral measurements performed in this study can be easily performed without destroying the target meteorite or touching its surface as long as it has a natural broken surface of a few millimeters in size. Along with the visible-range color photograph of meteorites, if their clasts or matrix has spectral data such as those measured in this study, those meteorites would be described in more detail, and researchers could have clearer ideas on which portion of which meteorite could be useful for their studies, significantly enhancing the value of the meteorite collection. The NIPR alone has more than 7000 classified meteorites, which include 187 carbonaceous chondrites, 216 HEDs, and 32 other achondrites such as ureilites and primitive achondrites. Applying the method employed here to these meteorite samples would yield useful spectroscopic and petrological information on them and their parent bodies such as Vesta, Vestoids, C-type asteroids, and other types of asteroids.

5. Summary

We have successfully demonstrated that VNIR spectral measurements of natural surface spots of Martian meteorites can give useful information on the rock types and mineral compositions of the measured spots. Our approach will be useful for both in-situ characterization of Martian rocks by a rover and non-destructive laboratory characterization of Martian meteorites. Compilation of such spectral data of Martian and other meteorites would also enhance the value of the meteorite collection and its database.

Acknowledgment

The Antarctic Martian meteorite samples studied here were kindly loaned from the National Institute of Polar Research (NIPR), and a Nakhla sample from the Natural History Museum. NASA/Keck RELAB is a multi-user facility which is supported by NASA

Planetary Geology and Geophysics Program and located at Brown University. This study was performed while T. H. was a visiting professor at the NIPR.

References

- Cloutis, E.A., Gaffey, M.J., 1991. Pyroxene spectroscopy revisited: spectral-compositional correlations and relationship to geothermometry. *J. Geophys. Res.* 96, 22809–22826.
- Dyar, M.D., Glotch, T.D., Lane, M.D., Wopenka, B., Tucker, J.M., Seaman, S.J., Marchand, G.J., Klima, R., Hiroi, T., Bishop, J.L., Pieters, C., Sunshine, J., 2011. Spectroscopy of Yamato 984028. *Polar Sci.* 4, 350–549.
- Greshake, A., Fritz, J., Stöffler, D., 2003. Petrography and shock metamorphism of the unique shergottite Yamato 980459 (abstract). International Symposium. Evolution of Solar System: a New Perspective from Antarctic Meteorites, 29–30, Nat. Inst. Polar Res., Tokyo.
- Greshake, A., Fritz, J., Stöffler, D., 2004. Petrology and shock metamorphism of the olivine-phyric shergottite Yamato 980459: evidence for a two-stage cooling and single-stage ejection history. *Geochim. Cosmochim. Acta* 68, 2359–2377.
- Ikeda, Y., 1997. Petrology and mineralogy of the Y-793605 Martian meteorite. *Antarct. Meteorite Res.* 10, 13–40.
- Ikeda, Y., 2003. Petrology of the Yamato 980459 shergottite (abstract). International Symposium. Evolution of Solar System: a New Perspective from Antarctic Meteorites, 42, Nat. Inst. Polar Res., Tokyo.
- Ikeda, Y., 2004. Petrology of the Yamato 980459 shergottite. *Antarct. Meteorite Res.* 17, 35–54.
- Imae, N., Ikeda, Y., Shinoda, K., Kojima, H., Iwata, N., 2003. Yamato nakhlites: petrography and mineralogy. *Antarct. Meteorite Res.* 16, 13–33.
- Koizumi, E., Mikouchi, T., McKay, G., Monkawa, A., Chokai, J., Miyamoto, M., 2004. Yamato 980459: crystallization of Martian magnesian magma. *Lunar Planet. Sci.* XXXV abstract #1494.
- Kojima, H., Miyamoto, M., Warren, P.H., 1997. The Yamato-793605 Martian meteorite consortium. *Antarct. Meteorite Res.* 10, 3–12.
- Lundberg, L.L., Crozaz, G., McSween, H.Y., 1990. Rare earth elements in minerals of the ALHA77005 shergottite and implications for its parent magma and crystallization history. *Geochim. Cosmochim. Acta* 54, 2535–2547.
- Ma, M.S., Laul, J.C., Schmitt, R.A., 1981. Complementary rare earth element patterns in unique achondrites, such as ALHA77005 and shergottites, and in the Earth. *Proc. Lunar Planet. Sci. Conf.* 12th, 1349–1358.
- Mason, B., 1981. ALHA77005 petrographic description. *Antarct. Meteorite Newsl.* 4 (1), 12. JSC Curator's Office, Houston.
- McSween, H.Y., Taylor, L.A., Stolper, E.M., 1979. Allan Hills 77005: a new meteorite type found in Antarctica. *Science* 204, 1201–1203.
- Mikouchi, T., Miyamoto, M., 1997. Yamato-793605: a new lherzolitic shergottite from the Japanese Antarctic meteorite collection. *Antarct. Meteorite Res.* 10, 41–60.
- Mikouchi, T., Koizumi, E., Monkawa, A., Ueda, Y., Miyamoto, M., 2003. Mineralogy and petrology of Yamato 000593: comparison with other Martian nakhlite meteorites. *Antarct. Meteorite Res.* 16, 34–57.
- Mikouchi, T., Koizumi, E., McKay, G., Monkawa, A., Ueda, Y., Chokai, J., Miyamoto, M., 2004. Yamato 980459: mineralogy and petrology of a new shergottite-related rock from Antarctica. *Antarct. Meteorite Res.* 17, 13–34.
- Pieters, C.M., 1983. Strength of mineral absorption features in the transmitted component of near-infrared reflected light: first results from RELAB. *J. Geophys. Res.* 88, 9534–9544.
- Pieters, C.M., Hiroi, T., 2004. RELAB (Reflectance Experiment Laboratory): a NASA multiuser spectroscopy facility. *Lunar Planet. Sci.* XXXV abstract #1720.
- Schueler, C.F., Blasius, K.R., Christensen, P., Silverman, S., Ruff, S., Wyatt, M., Mehall, G., Peralta, R.J., Bates, D., 2005. Mars exploration via thermal emission spectroscopy, in: Larar, A.M., Suzuki, M.; Tong, Q. (Eds), *Multispectral and Hyperspectral Remote Sensing Instruments and Applications II*, pp.318–324.
- Sunshine, J.M., Pieters, C.M., Pratt, S.F., 1990. Deconvolution of mineral absorption bands – an improved approach. *J. Geophys. Res.* 95, 6955–6966.
- Treiman, A.H., McKay, G.A., Bogard, D.D., Wang, M.S., Lipschutz, M.E., Mittlefehldt, D.W., Keller, L., Lindstrom, M.M., Garrison, D., 1994. Comparison of the LEW88516 and ALHA77005 Martian meteorites: similar but distinct. *Meteoritics* 29, 581–592.
- Ueda, Y., Miyamoto, M., Mikouchi, T., Hiroi, T., 2003. Reflectance spectra of the Yamato 000593 nakhlite: spectroscopic similarities to other nakhlites. *Antarct. Meteorite Res.* 16, 94–104.
- Wadhwa, M., McSween, H.Y., Crozaz, G., 1994. Petrogenesis of shergottite meteorites inferred from minor and trace element microdistributions. *Geochim. Cosmochim. Acta* 58, 4213–4229.

